HHS Public Access

Author manuscript

Mol Cell. Author manuscript; available in PMC 2018 August 03.

Published in final edited form as:

Mol Cell. 2017 August 03; 67(3): 498–511.e6. doi:10.1016/j.molcel.2017.06.024.

A PHOSPHOSITE WITHIN THE SH2 DOMAIN OF LCK REGULATES ITS ACTIVATION BY CD45

Adam H. Courtney[1], **Jeanine F. Amacher**[2], **Theresa A. Kadlecek**[3], **Marianne N. Mollenauer**[3], **Byron B. Au-Yeung**[1,4], **John Kuriyan**[2,3], and **Arthur Weiss**[1,3,5,*]

[1]Division of Rheumatology, Rosalind Russell and Ephraim P. Engleman Arthritis Research Center, Department of Medicine, University of California, San Francisco, CA, 94143, USA

[2]Departments of Molecular and Cell Biology, and Chemistry, University of California, Berkeley, CA, 94720, USA

[3]The Howard Hughes Medical Institute (HHMI)

SUMMARY

The Src Family kinase Lck sets a critical threshold for T cell activation because it phosphorylates the TCR complex and the Zap70 kinase. How a T cell controls the abundance of active Lck molecules remains poorly understood. We have identified an unappreciated role for a phosphosite, Y192, within the Lck SH2 domain which profoundly affects the amount of active Lck in cells. Notably, mutation of Y192 blocks critical TCR proximal signaling events and impairs thymocyte development in retrogenic mice. We determined that these defects are caused by hyperphosphorylation of the inhibitory C-terminal tail of Lck. Our findings reveal that modification of Y192 inhibits the ability of CD45 to associate with Lck in cells and dephosphorylate the C-terminal tail of Lck which prevents its adoption of an active open conformation. These results suggest a negative feedback loop which responds to signaling events that tune active Lck amounts and TCR sensitivity.

ETOC SUMMARY

Despite a critical requirement for Lck to initiate TCR signaling, how a T cell controls the abundance of active Lck molecules remains poorly understood. Courtney et al. report that a Lck phosphosite, Y192, when modified, can negatively regulate TCR signaling by preventing the phosphatase CD45 from activating Lck.

*correspondence: aweiss@medicine.ucsf.edu.

[4]Present address: Emory University, School of Medicine, Atlanta, GA, 30322, USA.

[5]Lead contact

AUTHOR CONTRIBUTIONS

A.C. and J.A. designed and performed experiments. M.M. assisted with experiments. T.K. and B.A. contributed reagents and expertise. A.C., J.A., J.K., and A.W. participated in experimental design, data analysis, and writing the manuscript.

Keywords

Lck; Src family kinase; T cell signaling; T cell antigen receptor; TCR; CD45; SH2 domain; phosphorylation; kinase; phosphatase

INTRODUCTION

Pathogenic microbes and malignant cells are neutralized by the immune system to prevent disease. T cells are essential to this capacity. T cells deploy a pathogen detector, the T cell antigen receptor (TCR), on their cell surface that binds antigens. Upon encountering antigen in the form of peptide-major histocompatibility complexes (pMHC), the TCR initiates a T cell response. Importantly, a T cell response requires the successful transmission of information across the plasma membrane. The kinase Lck converts an extracellular recognition event, TCR binding antigen, into a biochemical output, TCR complex phosphorylation. Specifically, Lck phosphorylates TCR-associated ζ- and CD3-chain tyrosine residues found within ITAM motifs that then recruit the effector kinase Zap70 to the plasma membrane where it also is phosphorylated by Lck (Chakraborty and Weiss, 2014; Smith-Garvin et al., 2009). Upon ITAM binding and phosphorylation, Zap70 is activated to phosphorylate the adaptor Lat and other regulators necessary to execute a T cell response. Because Lck is required to initiate TCR signaling, its activity must be tightly controlled.

Lck is a Src family kinase (SFK) and its activity in cells is controlled by two regulatory domains and several sites of post-translational modification (Figure 1A) (Boggon and Eck, 2004). Lck is anchored to the plasma membrane through lipidation of its N-terminus (Kabouridis et al., 1997). Adjacent to the membrane anchor is a motif that enables Lck to associate with the CD4 and CD8 coreceptors (Shaw et al., 1990). The activity of the catalytic kinase domain is governed by the SH2 and SH3 regulatory domains and two well-studied sites of tyrosine phosphorylation. Importantly, the SH2 and SH3 regulatory domains govern kinase activity by controlling the conformation of the kinase domain. Conformational regulation is achieved by phosphorylation of regulatory motifs within Lck (Figure 1B). Structures of the related SFKs Hck and Src reveal that binding of the SH2 regulatory domain to the phosphorylated C-terminal tail stabilizes the inactive autoinhibited conformation (Sicheri et al., 1997; Xu et al., 1997). In contrast, the active conformation of the catalytic kinase domain is stabilized through trans-autophosphorylation of the activation loop (Yamaguchi and Hendrickson, 1996). In this way, phosphorylation of Lck controls its conformation and therefore activity.

The protein tyrosine phosphatase CD45 dephosphorylates the inhibitory C-terminal tail of Lck. Loss of CD45 in T cells causes hyperphosphorylation of the inhibitory C-terminal tail which stabilizes the autoinhibited conformation and prevents trans-autophosphorylation of the activation loop (Mustelin et al., 1989; Ostergaard et al., 1989; Sieh et al., 1993). Therefore, loss of CD45 phosphatase activity drastically reduces the abundance of active Lck. Because Lck is predominately inactive when CD45 is absent, decreased TCR signaling is observed in CD45-deficient T cells and causes a block in thymocyte development in vivo (Kishihara et al., 1993; Koretzky et al., 1990; Pingel and Thomas, 1989). Despite the critical

requirement for CD45 in T cell function, how CD45 interacts with Lck to dephosphorylate its inhibitory tail is largely unknown. In contrast to CD45 deficiency, inhibition of the kinase that phosphorylates the inhibitory C-terminal tail of Lck, Csk, markedly increases active Lck abundance in resting T cells (Bergman et al., 1992; Nada et al., 1993; Schoenborn et al., 2011; Tan et al., 2014). Csk-deficiency in T cells causes abnormal thymocyte development, allowing the aberrant development of cells lacking a functional TCR (Schmedt et al., 1998). While both CD45 and Csk regulate Lck, it is unclear how their activities are coordinated to ensure the appropriate amount of active Lck in T cells.

The amount of active Lck impacts the initiation of TCR signaling. Using an allelic series to titrate CD45 expression, and thereby influence the amount of active Lck, TCR responsiveness correlated best with phosphorylation of the activation loop (Zikherman et al., 2010). Moreover, using small molecule inhibitors of Csk to increase active Lck abundance strikingly sensitizes the TCR to less abundant and lower affinity antigens (Manz et al., 2015). $CD8^+$ T cell subsets also appear to differ in their amounts of active Lck and capacity to signal through the TCR (Moogk et al., 2016). These observations together indicate that the amount of active Lck in a T cell sets an important threshold for TCR signaling. Yet how Lck activity is regulated and restrained to enforce a TCR signaling threshold is unclear.

The conventional view of SFK regulation has focused on two tyrosine phosphorylation sites: one activating (activation loop) and one inhibitory (C-terminal tail). We now report a critical role for a third site of tyrosine phosphorylation within the SH2 domain of Lck, Y192. Previously, we observed that this phosphosite was sensitive to Zap70 inhibition (Sjolin-Goodfellow et al., 2015). Because Zap70 is an Lck substrate, we speculated that phosphorylation of Y192 could participate in a negative feedback loop. Here, we present a negative feedback model for Lck wherein Y192 is phosphorylated in response to TCR signaling. Y192 is an underappreciated regulatory phosphosite conserved amongst all human SFKs (Figure 1A). ITK, a Tec family tyrosine kinase located downstream of Zap70, as well as Syk and Zap70, have previously been implicated in Y192 phosphorylation (Couture et al., 1996; Granum et al., 2014). Previous studies assessing the regulation of the SH2 domain of Lck have shown that mutation or phosphorylation of Y192 can alter its ligand specificity. However, our results suggest a significant additional role for Y192.

By analyzing the effects of Y192 mutation in the context of cells and purified proteins, we observe that Y192 directly governs access of the inhibitory C-terminal tail to the phosphatase CD45. As a consequence, Y192 variants profoundly affect TCR signaling due to altered levels of active cellular Lck and block thymocyte maturation in vivo. Our findings reveal a previously unappreciated mechanism for regulating the abundance of active Lck in T cells.

RESULTS

Mutation of Y192 Prevents Inducible TCR Signaling

We have previously described a genetically engineered system in which a mutant of Zap70 is inhibited by a small molecule ATP-competitive antagonist (Levin et al., 2008). Upon Zap70 inhibition, quantitative mass spectrometry analysis revealed a striking decrease in Lck

phosphorylation at Y192 (Sjolin-Goodfellow et al., 2015). Because Zap70 is a substrate of Lck, we reasoned that TCR signaling could regulate Lck activity through negative feedback (Figure 1C). Consistent with this hypothesis, increased phosphorylation of ζ-chain ITAMs, also Lck substrates, were observed upon Zap70 inhibition (Sjolin-Goodfellow et al., 2015). We therefore sought to determine whether modification of Lck Y192 influences TCR signaling.

Located within the SH2 domain of Lck, Y192 is conserved amongst human SFKs (Figure 1A). We speculated that phosphorylation of Y192 could create a binding site, for example allowing a negative regulator to dock; or conversely, disrupting a constitutive interaction between Lck and a positive regulator. Alternatively, mutation of Y192 has been suggested to alter the specificity of the SH2 domain, potentially influencing Lck interactions (Granum et al., 2014). To distinguish these possibilities, the impact of mutating the Y192 regulatory site on TCR signaling was evaluated. We tested the effects of installing a negative charge using glutamate and an alanine variant that lacks a negative charge but that is smaller in size. Finally, a phenylalanine variant was generated because it represents a conservative mutation that cannot be phosphorylated.

We stably expressed these constructs in an Lck-deficient Jurkat T cell line generated through CRISPR/Cas9 targeted deletion of Lck (Figures 1D & S1). Lck-deficient (J.Lck) cells reconstituted with WT Lck or Y192 variants were characterized for expression of key signaling proteins (Figure S1) and hallmarks of TCR signaling. An ideal readout of TCR stimulation is monitoring calcium changes because graded responses can be quantified in live cells. Upon stimulation by TCR crosslinking, Lck-deficient cells reconstituted with WT Lck exhibited a robust calcium response characterized by a large transient increase in intracellular calcium ion concentration followed by a decline (Figure 1E). In contrast, the parental J.Lck line, deficient for Lck, did not undergo a calcium increase following TCR stimulation because of the requirement for Lck to initiate TCR signaling. Interestingly, the Lck Y192F variant displayed a calcium response almost identical to WT Lck upon stimulation. Most striking, however, were the marked defects in calcium responses in cells expressing the Lck Y192E and Y192A variants. The Lck Y192E/A variants displayed markedly delayed and severely attenuated responses when compared to WT Lck (Figure 1E&F). Despite an inability to respond to TCR crosslinking, the Lck Y192E/A variants responded robustly to treatment with ionomycin which bypasses the requirement for TCR signaling (Figure S2).

To understand the defect in calcium response that occurs when Lck Y192 is mutated we monitored phosphorylation of signaling effectors. Total protein phosphotyrosine was assessed by immunoblot to reveal global changes in phosphorylation in response to TCR stimulation (Figure 2). A characteristic increase in the pattern of protein tyrosine phosphorylation occurred when Jurkat T cells are stimulated but not Lck-deficient J.Lck cells. In particular, induced phosphorylation of Zap70 and the ζ-chain could be observed following TCR stimulation. Consistent with the previously described calcium responses, J.Lck cells reconstituted with WT Lck and Lck Y192F displayed an inducible phosphorylation pattern similar to Jurkat T cells. Interestingly, cells reconstituted with Lck Y192E/A variants exhibited markedly attenuated induced protein tyrosine phosphorylation

when stimulated. Indeed, the phosphoprotein induction in the J.Lck Y192E/A variants appears more similar to Lck-deficient T cells with the exception of a prominent phosphoprotein near 56 kD, which is likely to be Lck.

To explore the mechanism of these defects further, we investigated specific signaling effectors by assessing known phosphorylation sites that activate them (Figure 2). We assessed PLCγ1 activation because it generates the secondary messengers that initiate the calcium response, as well as Erk activation (Smith-Garvin et al., 2009). PLCγ1 phosphorylation at the activating site Y783 was markedly impaired in the J.Lck cells expressing the Y192E/A variants, consistent with their defective calcium responses. The effector kinase Zap70 is required to initiate TCR signaling and therefore phosphorylation of PLCγ1 (Williams et al., 1999). Zap70 binds to the phosphorylated ITAM residues within the TCR complex, where the active conformation is stabilized by phosphorylation of the interdomain region (Y319) and activation loop (Y493) by Lck (Au-Yeung et al., 2009; Chan et al., 1995). Notably, in J.Lck cells reconstituted with WT or Lck Y192F we observed robust phosphorylation of Zap70 at both Y319 and Y493. Consistent with activation of Zap70 in these cells, an important Zap70 substrate Lat was robustly phosphorylated at Y191 (Zhang et al., 1998). In contrast, cells expressing Lck Y192E/A variants displayed a striking defect in both Zap70 phosphorylation, and consistent with its reduced activity, marked attenuation of Lat Y191 phosphorylation. The defects in early proximal signaling events in cells expressing Lck Y192E/A were also observed in Erk phosphorylation, which was delayed. In aggregate, the ability of TCR stimulation to induce phosphorylation of TCR signaling effectors and a subsequent calcium response were impaired by Y192 mutation.

Y192 Regulates Lck Activity and Tonic Signaling

Zap70 inhibition was previously observed to decrease Lck Y192 phosphorylation in both stimulated and resting cells. This observation suggests Y192 could regulate the abundance of active Lck in response to ongoing tonic TCR signaling that occurs prior to TCR stimulation (Sjolin-Goodfellow et al., 2015). Therefore, we postulated that phosphorylation of Y192 negatively regulates Lck in response to ongoing tonic TCR signaling (Figure 1C). In resting cells, tonic TCR signaling occurs in the absence of TCR ligand and is important for T cell survival (Polic et al., 2001; Seddon and Zamoyska, 2002). Because Lck activity is required for both tonic and inducible TCR signaling, we sought to assess the impact of Y192 on active Lck abundance and tonic signaling events (Figure 3A).

Phosphorylation of the inhibitory C-terminal tail (Y505), a modification that stabilizes the autoinhibited conformation of Lck, was similar in J.Lck cells reconstituted with WT Lck and Jurkat T cells (Figure 3B&C). However, when we compared phosphorylation at this site between Y192 variants we observed a surprising trend. The Lck Y192F variant displayed a slight increase in phosphorylation of the C-terminal tail, however, the more disruptive Y192E/A variants were hyperphosphorylated at this inhibitory site. Indeed, the Y192E/A variants displayed phosphorylation of the C-terminal tail comparable to cells deficient for CD45, the phosphatase that removes this modification. Correspondingly, for the Lck Y192E/A variants we observed a marked defect in phosphorylation of the activation loop (Y394), which stabilizes the active conformation. The striking 3-fold increase in inhibitory

C-terminal tail phosphorylation, and corresponding decrease in activation loop phosphorylation, indicate that Lck is autoinhibited and therefore inactive.

To demonstrate that the loss of active Lck observed with the Y192E/A variants is due to inhibitory regulation we treated cells with pervanadate, a general inhibitor of tyrosine phosphatases. By inhibiting tyrosine phosphatases, pervanadate causes the general activation of tyrosine kinases. Consistent with a functional kinase, pervanadate treatment caused robust autophosphorylation of the Lck Y192E/A variants and Lck-dependent cellular protein tyrosine phosphorylation (Figure S2B).

Because we predicted that Y192 modification could modulate tonic signaling, we monitored global protein tyrosine phosphorylation in resting cells. We observed a marked decrease in tonic signaling in the Lck Y192E/A variants as revealed by an overall reduction in phosphoprotein abundance (Figure 3D). Robust phosphorylation of Zap70 is associated with kinase activation which is induced by TCR stimulation. In resting T cells, however, basal levels of phosphorylated TCR ζ-chain and associated Zap70 can be detected (Di Bartolo et al., 1999; van Oers et al., 1994). Indeed, Zap70 phosphorylation was readily detected in resting Jurkat T cells in the absence of TCR engagement, and thereby serves as a read out of tonic TCR signaling (Figure 3B&E) (Levin et al., 2008). Cells expressing WT Lck or Y192F exhibit tonic signaling as revealed by Zap70 phosphorylation. In contrast, the Lck Y192E/A variants displayed a striking defect in tonic signaling highlighted by reduced overall protein tyrosine phosphorylation and a 6-fold reduction in Zap70 phosphorylation (Figure 3B,D&E). Because of the impact of Y192 perturbation on both tonic and inducible signaling we chose to investigate a physiological readout of these activities in vivo.

As a thymocyte matures in the thymus it displays a pre-TCR complex and SFK activity is required to phosphorylate its associated CD3 and ζ-chains. Without phosphorylation of the pre-TCR complex by SFKs Lck or Fyn in double negative ($CD4^-/CD8^-$) thymocytes, T cell development is arrested (van Oers et al., 1996). Loss of Lck and Fyn prevent a double negative thymocyte from progressing to the double positive ($CD4^+/CD8^+$) stage of development (Figure 4A). Once a thymocyte has become double positive, further Lck activity is required for its maturation. Specifically, a double positive thymocyte must undergo positive selection, whereby its TCR must induce a signal in response to self peptides (pMHC) for maturation to a single positive ($CD4^+$ or $CD8^+$) thymocyte. Loss of CD45, which markedly reduces the amount of active Lck, impairs pre-TCR signaling and positive selection causing an accumulation of double negative and double positive thymocytes (Figure 4A) (Byth et al., 1996; Kishihara et al., 1993). Because normal thymocyte maturation requires SFK activity, reconstitution of Lck/Fyn-deficient T cell progenitors affords a physiological measure of Lck activity in vivo (van Oers et al., 1996). We specifically employed Lck/Fyn-deficient T cells to abolish all SFK activity because Fyn can partially compensate for the loss of Lck. We reasoned that Fyn could obscure our ability to quantify thymocyte maturation as an in vivo readout of Lck activity. In contrast to Lck deficiency, the isolated loss of Fyn has little effect on thymocyte populations (van Oers et al., 1996). Therefore, Lck/Fyn-deficient hematopoetic progenitors were retrogenically reconstituted with either WT or Lck Y192E. To monitor viral reconstitution and Lck

expression our constructs contained a fluorescent protein (mCherry) that was liberated form Lck using a self-cleaving peptide (Szymczak et al., 2004) (Figure 4B).

Reconstituted progenitor cells were adoptively transferred into lethally irradiated mice and thymic repopulation was assessed after six weeks. Expression of WT Lck readily reconstituted development of CD4/CD8 double positive, and CD4 and CD8 single positive thymocytes. In contrast, mice reconstituted with the Lck Y192E variant displayed a marked defect in thymocyte development despite similar levels of Lck expression (Figure 4C & S3). Lck Y192E expression was unable to rescue the formation of CD4 or CD8 single positive thymocytes, but instead resulted in an accumulation of double negative and double positive thymocytes. Consistent with defects in thymocyte development in retrogenic mice expressing Lck Y192E, mature single positive T cells were also absent from the spleen. B cells do not typically express Lck and therefore do not require it for development; however, abundant retrogenic B cells ($B220^+$) were present consistent with successful engraftment (Figure 4D & S3). Because the Y192E variant causes a developmental defect similar to CD45-deficiency, this finding is consistent with reduced active Lck (Byth et al., 1996; Kishihara et al., 1993). Overall, our findings reveal that the Y192 phosphosite can alter physiologically important TCR signaling and impacts thymocyte maturation.

Lck Y192 Variants Prevent CD45-Mediated Activation of Lck Independently of SH2 Phosphopeptide Affinity

The defects in signaling caused by Y192 perturbation in J.Lck cells and thymocyte maturation in retrogenic mice are strikingly similar to the phenotype of CD45-deficiency (Figures 3B & 4). Because Lck is a CD45 substrate, mutation of Y192 may disrupt the ability of CD45 to dephosphorylate Lck. To test our prediction, we developed a reconstituted cellular system for the CD45-mediated regulatable activation of Lck. To regulate Lck activation, Lck and CD45 were expressed in HEK 293 cells with an analog-sensitive allele of Csk (Csk^{AS}) which is inhibited by the small molecule 3-IB-PP1 (Schoenborn et al., 2011). Because Csk phosphorylates the inhibitory C-terminal tail, inhibition of Csk^{AS} with 3-IB-PP1 treatment should result in acute CD45-mediated dephosphorylation of this site. Lastly, as a readout of Lck kinase activity we included an Lck substrate, chimeric CD8/ζ-chain (Figure 5A). We reasoned that defects in Lck dephosphorylation would indicate whether mutation of Y192 disrupts the ability of CD45 to activate Lck.

Upon Csk^{AS} inhibition by 3-IB-PP1 treatment, dephosphorylation of the C-terminal tail (Y505) on WT Lck occurs. Because active Lck abundance is increased, the CD8/ζ-chain is phosphorylated (Figure 5B&C). Similar to WT Lck, we observed that the Y192F mutant is dephosphorylated by CD45 and CD8/ζ-chain phosphorylation is increased, albeit to a lesser extent. In contrast, when we examined the Lck Y192E/A variants, the ability of CD45 to dephosphorylate the C-terminal tail upon Csk^{AS} inhibition was markedly impaired. Because the Y192E/A variants are resistant to dephosphorylation and activation, only a minimal increase in CD8/ζ-chain phosphorylation occurred.

Our results using a reconstituted system suggest that the SH2 domain of Lck mediates recognition by CD45. Previous investigations revealed that mutation or phosphorylation of Y192 has the potential to affect the affinity or specificity of the SH2 domain (Couture et al.,

1996; Granum et al., 2014; Jin et al., 2015; Stover et al., 1996). One potential mode of SH2-dependent regulation would be the accessibility of the phosphorylated C-terminal tail (Model 1, Figure S4).

Therefore, we tested whether mutation of Lck Y192 could increase the affinity of the SH2 domain for the phosphorylated C-terminal tail. Such an increase in affinity could protect it from CD45 (Nika et al., 2007). However, isothermal titration calorimetry (ITC) experiments previously showed that although affinity of the Lck SH2 domain for a variety of ligands does vary for the Y192E variant, this is not the case for a phosphopeptide derived from the C-terminal tail (Granum et al., 2014). Similarly, we noticed only a slight decrease in Lck Y192E SH2 binding affinity for the C-terminal tail phosphopeptide and a higher affinity variant (YQPQP to YQEIP) (Figure S5A). Together these observations are contradictory to a model where mutation of Y192 causes the SH2 domain to protect the phosphorylated C-terminal tail through enhanced binding.

Disruption of a Y192 Interaction Site Protects the Inhibitory C-terminal Tail

We next explored whether there was a direct functional interaction between CD45 and Lck that is influenced by Y192 (Model 2, Figure S4). We expressed and purified WT and Y192E Lck, as well as the cytoplasmic domain of CD45. Incubation of Lck with ATP, followed by immunoblot and mass spectrometry, revealed that Lck robustly phosphorylates itself and CD45 in vitro. In particular, the activation loop (Y394), C-terminal tail (Y505), as well as additional tyrosines are phosphorylated (Table S1). To test the ability of CD45 to dephosphorylate the C-terminal tail, we allowed Lck to autophosphorylate itself and then added the SFK-specific inhibitor PP1, and CD45. Indeed, the C-terminal tail is robustly dephosphorylated; however, the Y192E variant is resistant to dephosphorylation, recapitulating our cell-based findings (Figure 6A).

To remove the need for Lck to first autophosphorylate itself (which results in phosphorylation of multiple residues in CD45 and Lck), we generated a kinase inactive Lck variant (D364N); however, this protein aggregated when purified in *E. coli*. Therefore, we tested whether Hck could substitute for Lck. Hck is a close relative of Lck and assessing it would broaden our findings to an additional SFK that is also a CD45 substrate (Zhu et al., 2011). Overall, Hck and Lck are 72% identical in sequence and the tail peptides vary by only a single residue. Importantly, the Lck Y192 phosphosite is conserved in Hck (Y209). Similar to our results with the Lck SH2 domains, we observed an approximately 3-fold decrease in the Hck SH2 Y209E binding to several tail-related phosphopeptides, again consistent with prior observations (Figure S5B) (Granum et al., 2014). These results provide additional confirmation that increased protection by the SH2 domain is not conferring resistance to CD45-mediated dephosphorylation.

A kinase-inactive Hck variant (D381N) was stable and expressed well in bacteria. Uniform phosphorylation of the Hck C-terminal tail (Y522) was achieved through co-expression of Csk. An additional variant was generated that incorporates both D381N and the Y209E SH2 domain mutation. Importantly, Hck D381N and Y209E/D381N experiments revealed similar SH2-dependent regulation of CD45 dephosphorylation of the C-terminal inhibitory tyrosine seen using Lck protein, whereby the Y209E variant is resistant to dephosphorylation (Figure

6B). In addition, we tested Y209F and Y209A Hck variants, which recapitulated our cell based results (Figure S5C). Interestingly, we do not see a noticeable difference in dephosphorylation rate between the D381N and Y209E/D381N Hck variants when using the promiscuous bacterial Yersinia protein tyrosine phosphatase YopH, suggesting the effect of the SH2 mutation is CD45-specific (Figure 6C). Similarly, removing the capacity of the SH2 domain to bind the phosphorylated C-terminal tail abolishes the resistance of the Y209E variant to CD45-mediated dephosphorylation (Figure S5D).

Taken together, our results indicate that mutations within the SH2 domain (Lck Y192 or Hck Y209) can impair the ability of CD45 to recognize its substrate, consistent with our proposed Model 2 (Figure S4). Next, we sought to assess whether Y192 could comprise a potential interaction site. Consistent with this reasoning, residues adjacent to Y192, including a nearby loop that extends from the central β-sheet, are well conserved (Figure 7A) (Ashkenazy et al., 2010; Tong et al., 1996). It is possible that these residues are conserved because they contribute to peptide binding, or alternatively, are indicative of a CD45 docking site.

We therefore sought to evaluate the functional consequences of disrupting this putative interaction site in a steady-state dephosphorylation assay (Figure 7B). Kinase inactive (K273R) Lck was expressed in HEK 293 cells where its C-terminal tail is robustly phosphorylated by endogenous Csk. CD45 was also expressed and the extent to which it dephosphorylated the C-terminal tail (Y505) of Lck was assessed by immunoblot (Figure 7C). As expected, the Y192E variant was hyperphosphorylated, and consistent with a docking site, several additional variants displayed varying degrees of protection from CD45-mediated dephosphorylation.

A Y192-Dependent Docking Site is Necessary for Association of Lck with CD45 in Cells

We next determined whether the putative docking site mediates association between Lck and CD45 in cells. An interaction between the SH2 domain of Lck and CD45 has been previously reported, therefore we evaluated whether Y192 could influence an interaction between Lck and CD45 (Ng et al., 1996). We immunoprecipitated CD45 from J.Lck cells stably expressing Lck Y192 variants (Figure 7D). The extent to which Lck was associated with CD45 following immunoprecipitation was assessed by immunoblot. Consistent with a docking site, WT Lck was associated with CD45; however, the Y192 variants exhibited impaired association. Interestingly, the Y192F variant, despite reconstituting signaling events, also displayed reduced association with CD45.

To eliminate the influences of Lck autophosphorylation and CD45 phosphatase activity, we expressed kinase inactive Lck (K273R) and phosphatase inactive CD45 (C828S) in HEK 293 cells. Using this approach, we observed a similar trend as with the J.Lck cells (Figure 7E). Interestingly, we observed that the Y192F variant displayed intermediate association with CD45, consistent with this mutation causing a modest reduction in CD45-mediated dephosphorylation of the C-terminal tail (Figures 3 & 5). Moreover, several nearby residues that affect dephosphorylation also disrupt association of Lck with CD45 (Figure 7B & S6).

We next sought to assess whether autoinhibited or open Lck associated more favorably with CD45 (Figure 7F). The autoinhibited conformation was stabilized by mutating the C-terminal tail to a more optimal sequence for binding to the inhibitory SH2 domain (YQPQP to YQEIP, denoted hereafter as “QEI”) (Figure S5) (Nika et al., 2007). Disruption of autoinhibition was achieved by disabling SH2 binding (R154K) or preventing phosphorylation (Y505F). We found that the capacity of Lck to associate with CD45 was, indeed, sensitive to its conformation. Disrupting autoinhibition (R154K and Y505F) markedly increased the ability of Lck to associate with CD45, whereas stabilizing autoinhibition (QEI) reduced association. Interestingly, the Y192E variant disrupted association regardless of conformation. To our surprise, association of Lck with CD45 in cells did not appear to be dependent on phosphorylation of the C-terminal tail, as revealed by the Y505F variant.

Overall our findings indicate that the Y192 phosphosite resides within a conserved region of the SH2 domain that influences the association of Lck with CD45 and dephosphorylation of the C-terminal tail.

DISCUSSION

Mounting evidence indicates that TCR signaling is critically sensitive to the amount of active Lck. In resting T cells a significant population of Lck is in the active conformation (Nika et al., 2010). Consistent with the presence of active Lck in resting T cells, TCR ζ-chain phosphorylation can be detected in ex-vivo thymocytes and in peripheral T cells (van Oers et al., 1994; Zikherman et al., 2010). It is believed that TCR low affinity interactions with endogenous pMHC influence the extent of ζ-chain phosphorylation (Mandl et al., 2013; Persaud et al., 2014). CD45 expression is required for this basal ζ-chain phosphorylation, presumably to provide for an active pool of Lck (Zikherman et al., 2010). Because a proportion of Lck is active in resting thymocytes and T cells, it has been suggested that changes in the amount of active Lck are not required to initiate TCR signaling, but these findings remain controversial (Ballek et al., 2015; Nika et al., 2010; Philipsen et al., 2017; Stirnweiss et al., 2013). However, it is known that the amount of active Lck in a T cell can determine whether it responds to antigen or not (Manz et al., 2015; Zikherman et al., 2010). Regulatory feedback loops are therefore predicted to govern the amount of active Lck.

Previously seen changes in Lck phosphorylation upon inhibition of Zap70 suggested to us that downstream kinases may directly impact Lck activity. In particular, when Zap70 was inhibited we previously observed an increase in activation loop Y394 phosphorylation, increased ITAM phosphorylation, and a striking decrease in phosphorylation of a third tyrosine residue within the SH2 domain, Y192 (Sjolin-Goodfellow et al., 2015). Consistent with a critical regulatory role, we have found that mutation of Y192 blocks both inducible and tonic TCR signaling in Jurkat T cells. Interestingly, we found that this inhibition of TCR signaling is due to hyperphosphorylation of the inhibitory C-terminal tail of Lck. The observed block in Lck activity caused by mutation of Lck Y192 is strikingly similar to the phenotype of CD45-deficiency in cells and mice (Byth et al., 1996; Ostergaard et al., 1989).

Consistent with these observations, we demonstrate using reconstituted systems that modification of Y192 profoundly disrupts the ability of CD45 to activate Lck.

Lck is a CD45 substrate and therefore CD45 must interact with autoinhibited Lck to dephosphorylate it. However, it is unclear whether the capacity of CD45 to recognize and dephosphorylate Lck is mediated solely through recognition of the phosphorylated C-terminal tail (Model 1, Figure S4). Previous studies using in vitro binding studies have shown that mutation or phosphorylation of Y192, or the equivalent residue in other SFKs, can alter SH2 domain specificity (Couture et al., 1996; Granum et al., 2014; Jin et al., 2015; Stover et al., 1996). An increase in affinity of the SH2 domain for the phosphorylated tail residue could protect this site; however, this was not the case for the Y192 variants we tested (Figures S4 and S5). Alternatively, it has been proposed that CD45 can become phosphorylated on Y1193 and be bound by the SH2 domain of Lck (Autero et al., 1994). However, we mutated this putative phosphorylation site within CD45 and saw no effect on function (data not shown).

Protein phosphatases can achieve selectivity by docking with specific sites on their substrates (Li et al., 2014; Ragusa et al., 2010). Interestingly, the capacity of the SH2 domain of Lck to interact with CD45 has been previously reported (Ng et al., 1996). We therefore explored whether CD45 docks with Lck to facilitate dephosphorylation of the C-terminal tail (Model 2, Figure S4). Our findings confirm an interaction between Lck and CD45 and that it is Y192-dependent. Moreover, our findings reveal that CD45 associates more readily with Lck in its open conformation. One possibility is that by binding to the open conformation of Lck, CD45 stabilizes Lck in a state where its C-terminal tail is accessible. This is consistent with the observation that if both CD45-SH2 docking and SH2-phosphotyrosine binding are disrupted, CD45 can readily dephosphorylate the C-terminal tail (Figure S5). It remains to be determined how association of Lck with CD45 facilitates access to the phosphorylated C-terminal tail mechanistically and what region of CD45 participates in this interaction. Our findings also do not exclude the possibility that phosphorylation of Y192 regulates Lck function in additional ways, such as through altered SH2 binding (Couture et al., 1996; Granum et al., 2014). Despite these questions, our findings demonstrate that modification of Y192 and adjacent residues disrupts the ability of CD45 to associate with Lck and activate it which profoundly inhibits TCR signaling.

The Lck Y192 phosphosite has been known for over twenty years and responds to TCR stimulation, between 5–10% of Lck is reportedly phosphorylated at this site (Couture et al., 1996; Granum et al., 2014; Soula et al., 1993). The physiological importance of the Y192 phosphosite is highlighted by our observation that thymocyte development is blocked in retrogenic mice harboring a Y192 mutation. Our findings suggest that in response to Y192 phosphorylation, the ability of CD45 to dephosphorylate the inhibitory C-terminal tail of Lck is diminished and therefore the amount of active Lck is reduced (Figure S7). These observations are consistent with a negative feedback loop. Although the exact details are unknown, there are a number of candidate kinases that could directly regulate phosphorylation of Y192. Our prior study suggests that phosphorylation of Y192 is Zap70-dependent (Sjolin-Goodfellow et al., 2015). Consistent with this, the kinase ITK, which is downstream of Zap70, has been reported to modify this site (Granum et al., 2014).

An important feature of the putative Y192-dependent feedback loop is that while the association of Lck with CD45 is disrupted the catalytic activity of CD45 is unaffected. Such a mechanism confers specificity, negatively regulating the activation of Lck while leaving other potential targets of CD45 intact. Among other reported substrates are the activation loop of Lck and the signaling motifs in the TCR ζ-chain. In both these cases CD45 exerts a negative effect on TCR signaling. Therefore, a negative feedback loop that phosphorylates Y192 can reduce TCR signaling by disrupting the ability of CD45 to activate Lck while preserving the ability of CD45 to dephosphorylate the TCR ζ-chain. In this way, Lck function and TCR signaling are inhibited.

STAR METHODS

CONTACT FOR REAGENT AND RESOURCE SHARING

Further information and requests for reagents may be directed to the corresponding author, Arthur Weiss (aweiss@medicine.ucsf.edu).

EXPERIMENTAL MODEL AND SUBJECT DETAILS

Mice—Mice were maintained on the C57BL/6 genetic background. BoyJ mice were used as congenic hosts (CD45.2) for adoptive transfer studies. Mice were used at 4–10 weeks of age. All mice were housed in a specific pathogen free facility at UCSF according to the University Animal Care Committee and NIH guidelines.

Cell lines—Jurkat T cells (a human male leukemic T cell line) were maintained by the Weiss lab and are routinely stained for the expression of CD3 or TCRβ and other surface markers. Cells were maintained in a tissue culture incubator at 37 °C with 5% CO_2 in RPMI culture medium supplemented with 10% fetal bovine serum and glutamine (2 mM). Jurkat variants deficient for specific proteins of interest were generated using CRISPR/Cas9 targeted gene deletion. Genomic regions targeted by CRISPR/Cas9 were sequenced to confirm disruption of the coding sequence and loss of the protein product validated by immunoblot or flow cytometry. Cell lines that were reconstituted with Lck were confirmed by immunoblot and specific mutations validated by sequencing the PCR amplified construct from genomic DNA. HEK 293 cells were obtained from the ATCC (gender not provided) and maintained in DMEM supplemented with 10% fetal bovine serum and glutamine (2 mM) under culture conditions similar to those described for Jurkat T cells.

METHOD DETAILS

Targeted deletion of Lck and CD45—Lck and CD45-deficient cell lines were generated by transiently expressing both Cas9 and a guide RNA against Lck or CD45. Guide RNAs were generated by cloning of oligonucleotide targeting sequences into the pX330 vector (Cong et al., 2013). Constructs were electroporated into Jurkat T cells and single clones expanded by either single cell sorting or limiting dilution. Expanded clones were screened for expression of Lck and CD45. Reconstituted Lck-deficient (J.Lck) lines were generated by electroporating J.Lck cells with a pEF vector to express WT Lck or Y192 variants followed by selection with Blasticidin (10 μg/mL). Individual clones were isolated

using limiting dilution. Expanded clones were assessed for expression of Lck, CD45 and CD3.

Intracellular calcium measurements—Cells were rinsed and resuspended in RPMI supplemented with 5% FBS and 10 mM HEPEs at 10^7 cells/mL. Cells were loaded at 37 °C with Indo-1 AM (1 μg/mL) for 40 minutes. Cells were rinsed twice and resuspended in medium at 5×10^6 cells/mL. Cells were maintained at 37 °C and analyzed on a BD Fortessa flow cytometer. A 40 second baseline was collected prior to stimulation with anti-TCR antibody (C305, 0.85 μg/mL). Ionomycin treatment was used as a positive positive control. Ratio of calcium bound:unbound was calculated using FlowJo software. Responses were quantified from three experiments using the area under curve (AUC) function of PrismGraph.

Immunoblotting—Cells were rinsed with RPMI and resuspended at 5×10^6 cells/mL and rested for 15 minutes at 37 °C. Cells were either left unstimulated or treated with anti-TCR antibody (C305, 0.85 ug/mL), or pervanadate (100 μM). Reconstituted HEK 293 cells were treated with either DMSO or 3-IB-PP1 (5 μM). Cells were then lysed through addition of NP-40 lysis buffer to a final concentration of 1% containing inhibitors: $NaVO_4$ (2 mM), NaF (10 mM), EDTA (5 mM), PMSF (2 mM), Aprotinin (10 μg/mL), Pepstatin (1 μg/mL), Leupeptin (1 μg/mL), and PP2 (25 μM). Lysates were placed on ice and debris pelleted at 13,000 × g. Supernatant was run on 4–12% NuPage or 10% Bis-Tris gels and transferred to PVDF membranes. Membranes were blocked using TBS-T and BSA, and then probed with primary antibodies overnight at 4 °C. The following day blots were rinsed and incubated with HRP-conjugated secondary antibodies. Blots were detected using chemiluminescent substrate and a BioRad Chemi-Doc imaging system. Quantification was performed using Image Lab software.

Lentivirus preparation—Murine WT and Y192E Lck were cloned into the pHR backbone under the expression of an EF1α promoter. A C-terminal P2A self-cleaving peptide followed by mCherry was incorporated to assess transduction efficiency and expression levels. Packaging vector pCMV dR8.91, envelope vector pMD 2.G, and pHR Lck constructs were transiently co-transfected into LX-293T cells using TransIT-LT1 reagent (Mirus). Media was replaced the following morning and viral supernatants collected every day for two days. A solution of 25% PEG 8000 in PBS was added to a final concentration of 5% and virus precipitated overnight at 4 °C. The following data virus particles were pelleted and resuspended in culture medium.

Retrogenic mice—Bone marrow was harvested from 4–10 week old *Lck/Fyn*$^{-/-}$ mice on the C57BL/6 genetic background and depleted of lineage positive cells using a hematopoetic stem cell isolation kit (Stem Cell Technologies). Lineage negative cells were stained for c-Kit and Sca1 on ice prior to sorting with a BD FACs Aria cell sorter. Progenitor cells were collected (lineage negative, c-Kit+, Sca1$^+$) and cultured overnight in complete medium supplemented with IL-3 (20 ng/mL), IL-6 (50 ng/mL) and stem cell factor (SCF) (50 ng/mL). The following day wells were coated with of Retronetin (40 μg/mL) in PBS for 2 hours in a non-TC treated 96-well plate. Wells were rinsed with PBS and blocked briefly with

complete media before adding concentrated virus. Virus harvested from one 10 cm dish was split between 4–5 wells. Virus was spun at 2500 RPM for 2 hours at room temperature prior to adding ≈10^5 *Lck/Fyn*$^{-/-}$ progenitors per well. Cells were then spun at 1200 RPM for 30 minutes before culturing over night at 37 °C. The following day mCherry levels were assessed by FACs to determine transduction efficiency. Transduced cells were rinsed twice and resuspended in PBS and 25, 000 cells were injected into lethally irradiated 4–8 week old BoyJ (CD45.1) recipients. Thymus and spleen were harvested and analyzed after 6 weeks. All mice were housed in a specific pathogen free facility at UCSF according to the University Animal Care Committee and NIH guidelines.

To confirm mCherry expression, BoyJ recipients were bleed at 5 weeks post-injection. Thymus and spleen were harvested at 6 weeks and ruptured over a 0.45 μm mesh and washed with FACs buffer (PBS with 2% FBS and 2 mM EDTA). Red blood cells were removed by ACK lysis and washed twice with FACs buffer. Thymocytes were stained on ice with antibodies against CD45.2, CD4, CD8, CD25, CD44 and DAPI. Splenocyes were similarly stained with DAPI, CD45.2, CD4, CD8, pan-NK, B220 and DAPI. Samples were collected on a BD Fortessa flow cytometer and data analyzed using FlowJo software. Retrogenic cells were identified as CD45.2$^+$/mCherry$^+$. N=5–6 mice were analyzed for each construct (WT Lck versus Lck Y192E).

Reconstituted system for Lck activation—HEK 293 cells were transfected at ≈ 60% confluency with the following constructs: pEF CD45 (1.5 μg), pEF Csk^{AS} (membrane anchored)(2 μg), CD8/ζ (0.3 μg), pEF Lck (0.2 μg), and empty pEF vector to 4 μg of total DNA per well (6-well plate). Plasmids were combined in Opti-mem medium before addition of Lipofectamine 2000 (ThermoFisher) (10 uL per 4 μg of DNA) as per manufacturer's instructions. Plasmids were then added to cells for 4 hours before adding full medium and culturing overnight. After 24 hrs cells were harvested and rinsed, and then resuspended in DMEM medium. Cells were incubated at 37 °C for 15 minutes then treated with 3-IB-PP1 (5 μM) for 1 min and then lysed on ice. The Csk^{AS} and CD8/ζ constructs, and 3-IB-PP1 inhibitor have been previously described (Chan et al., 1991; Schoenborn et al., 2011; Tan et al., 2014).

Immunoprecipitation—Anti-CD45 antibody (9.4) was conjugated to protein A agarose and rinsed twice with 0.2 M sodium borate (pH 9.0). The resin was then resuspended in borate buffer and solid dimethylpimelimidate (DMP) added to a concentration of 20 mM. The resin was then incubated for 30 minutes at room temperature with mixing and then rinsed with 0.2 M ethanolamine (pH 8.0). The resin was then incubated with ethanolamine for 30 minutes and washed twice with TBS and stored at 4 °C as a 50% slurry. Prior to immunoprecipitation resin was rinsed with wash buffer (0.1% NP-40 TBS). Cells were incubated at 37 °C in serum-free medium and then pelleted at room temperature. Jurkat T cells 1–2 × 10^7 cells were used and for HEK 293 cells 2–3 × 10^6 cells. 400 uL of Ice cold lysis buffer (1% NP-40 TBS pH 7.4 supplemented with $NaVO_4$ (2 mM), NaF (10 mM), EDTA (5 mM), PMSF (2 mM), Aprotinin (10 μg/mL), Pepstatin (1 μg/mL), Leupeptin (1 μg/mL)) was added to the cell pellet and vortexed before placing on ice. Samples were kept on ice for 10 minutes prior to centrifugation at 13,000 g for 10 minutes to pellet cell debris. A

small aliquot was removed from each sample prior to immunoprecipitation (WCL). The remaining lysate was transferred to a fresh tube and 75 μL of anti-CD45 resin (50% slurry) was added. Samples were incubated for 2 hours at 4 °C before pelleting the resin and rinsing 3x with ice cold wash buffer in a refrigerated microfuge. Captured proteins were eluted by adding SDS sample buffer to the resin and incubating 5 minutes. J.Lck cells were electroporated with 10 μg of vector DNA using a BioRad Gene Pulser Xcell. 15×10^6 cells were resuspended in 400 μL of RPMI per electroporation in a cuvette (0.4 μm gap). Cells were then recovered in full medium for 2 days prior to immunoprecipitation. Quantification of band intensity following immunoblot was carried out using ImageLab software and denoted as a ratio of immunoprecipitated Lck to CD45. Note: Jurkat T cells express several isoforms of CD45 which is a large glycoprotein. Because transferring CD45 to a membrane during blotting can be inconsistent, the ratio of Lck/CD45 may underrepresent the actual extent of defects in Lck association.

In vitro desphosphorylation assays—Unless otherwise specified, all assays were conducted in multi-well plate format using 1 μM Hck/Lck and CD45 at a 1:1 ratio in buffer (25 mM Tris pH 8.0, 50 mM NaCl, 10% (*w/v*) glycerol, 0.5 mM TCEP). For assays involving Lck, 50 μM ATP and 250 μM $MgCl_2$ were added approximately 1h before the start of the dephosphorylation reaction in order to phosphorylate the protein. Approximately 5 min before CD45 addition, the reaction was quenched using 200 nM PP1 inhibitor, introducing <0.1% (*v/v*) DMSO. Dephosphorylation was assessed by immunoblotting with anti-Lck pY505. The antibody was successful for the conserved tails of both Lck and Hck. Immunoblots were quantified using ImageJ, and a consistent CD45 concentration in each sample was validated by coomassie staining.

Fluorescence polarization assays—Hck constructs. FITC conjugated peptides corresponding to the phosphorylated C-terminal tail of Lck and Hck and variants were synthesized and purified to >90% by HPLC (Biomatik). FP assays were conducted as described previously (Amacher et al., 2014), using the following buffer: 25 mM Tris pH 8.0, 50 mM NaCl, 10% (*w/v*) glycerol, 0.5 mM TCEP. Briefly, K_d values were determined by adding 30 nM fluorescein-labeled peptide to a 3-fold dilution series of WT or Y209E Hck SH2 protein. K_d values were determined as previously described (Vouilleme et al., 2010).

Lck constructs. GST Lck SH2 protein was added to HEPEs buffer (20 mM HEPEs, 150 mM NaCl, pH 7.4) containing 2 mM DTT. An equal volume of the fluorescence polarization probe (FITC-TEGQ[pY]QPQP) was combined 1:1 to a final concentration of 200 nM. Data were plotted as a ratio of peptide bound:total peptide versus protein concentration and analyzed as with Hck SH2 domains.

Protein Purification—Hck and CD45 purification. Human Hck proteins (D381N, Y209E/D381N, and D381N/EEI, residues 81-526, KD-tail D381N, residues 246-526, and SH2 variants, residues 135-242), human CD45 ICM (WT and trapping mutants, D819A and C851S, residues 598-1304), and YopH were expressed in BL21 (DE3) *E. coli* cells with an N-terminal His_6 tag. In the Hck D381N, Y209E/D381N, and D381N/EEI constructs, the His-tag was followed by a PreScission protease recognition sequence, whereas a cleavable SUMO tag preceded Hck SH2 and CD45 proteins. Hck D381N, Y209E/D381N, D381N/

EEI, and KD-tail proteins were co-expressed with human Csk (GST-tagged, residues 1-450), and phosphorylation of Y522 was assessed by immunoblot. Following induction with IPTG, protein was expressed for approximately 18 hours at 18°C. Hck and CD45 varian ts were purified by immobilized metal-affinity, anion exchange, and size exclusion chromatography. The cells were collected by centrifugation and resuspended in 2x lysis buffer (50 mM Tris pH 8.5, 200 mM NaCl, 10mM $CaCl_2$, 10mM $MgCl_2$, 20% (*w/v*) glycerol, 50 mM imidazole pH 8.5, 0.25 mM TCEP, DNAse, protease inhibitor cocktail). Following lysis by high pressure cell homogenization, cells were spun at 17K rpm for 1h. The supernatant was then collected, filtered, and loaded onto a 5 mL His-trap NiNTA column (GE Lifesciences). The column was then washed with NiNTA A buffer (25 mM Tris pH 8.5, 250 mM NaCl, 10% (*w/v*) glycerol, 25 mM imidazole pH 8.5, 0.25 mM TCEP) for approximately 5 column volumes (CV), followed by 12 CV of Q_A buffer (25 mM Tris pH 8.5, 50 mM NaCl, 10% (*w/v*) glycerol, 0.5mM TCEP) + 10 mM imidazole pH 8.5. Protein was eluted from the NiNTA column directly onto an anion exchange Q column using NiNTA B buffer (25 mM Tris pH 8.5, 50 mM NaCl, 10% (*w/v*) glycerol, 400 mM imidazole pH 8.5, 0.25 mM TCEP). The protein was then eluted in a gradient of Q_B buffer (25 mM Tris pH 8.5, 1 M NaCl, 10% (*w/v*) glycerol, 0.5 mM TCEP). CD45 and SH2 proteins were cleaved using the SUMO protease, ULP-1, and subjected to a subtractive NiNTA column (same buffers as above, wash buffer: Q_A + 10 mM imidazole pH 8.5 and elution buffer: NiNTA B). The storage buffer used for size exclusion chromatograph (Superdex S200, GE Lifesciences) contained 25 mM Tris pH 8.5, 150 mM NaCl, 10% (*w/v*) glycerol, 0.5 mM TCEP. Protein was then concentrated to ≈0.3–2 mM, and flash frozen in liquid nitrogen for storage at −80°C.

Lck purification. WT and Y192E Lck proteins (*Mus musculus*, residues 43-509) were expressed in SF9 insect cells with an N-terminal His_6 tag followed by a SUMO protein tag. Lck purification followed an identical protocol as described above, with the following differences: lysed cells were spun at 40K rpm for 1 hr, and the buffers were made with Tris pH 8.0.

Lck SH2 domain purification. SH2 domains from human Lck (residues 123-227) were expressed as GST fusions using the pGEX vector in *E. coli* (BL-21 pLys). Single colonies were used to inoculate a starter culture containing LB broth and ampicillin (100 μg/mL) and cultured overnight. The starter culture was used to inoculate a 600 mL culture which was grown at 37 °C and shaken at 225 RPM until an O.D. 600 nm of 0.6 was reached. The culture was then induced with 0.3 mM IPTG and cultured overnight at 18 °C at 225 RPM. The cultures were then pelleted and frozen at −80 °C. Pellets were thawed on ice and resuspended in lysis buffer (20 mM HEPEs, 140 mM NaCl, 10 mM DTT, 5 mM EDTA, 1 mM PMSF, 1% NP-40, pH 7.2) and sonicated on ice. Lysate was then centrifuged at 30K g for 45 minutes to remove debris and filtered through a 0.45 μm membrane. GST SH2 fusions were purified using a GST Trap 4B column (GE Healthcare). The column was washed extensively with wash buffer (20 mM Hepes, 140 mM NaCl, 5 mM EDTA, 5 mM DTT pH 7.2) followed by elution buffer (20 mM HEPEs, 140 mM NaCl, 5 mM EDTA, 10 mM DTT, 10 mM Glutathione, pH 7.2). Fractions were collected and analyzed by SDS-PAGE. Fractions containing GST SH2 fusions were combined and frozen in liquid nitrogen.

Lck SH2 homology analysis—Sequence conservation of the Lck SH2 domain was mapped to the the phosphopeptide bound structure of the SH2 domain (PDB 1LKK) (Tong et al., 1996). For the analysis, 150 homologs with between 95% and 25% sequence conservation were aligned using the Consurf server (Ashkenazy et al., 2010).

QUANTIFICATION AND STATISTICAL ANALYSIS

For experiments using cell lines, each experiment was independently replicated at least 3 times unless otherwise stated (N=3). Each replicate was performed on separate days and analyzed independently. For immunoblots, band intensity was quantified using Image Lab and normalized to WT. For intracellular calcium ion measurements, the area under the curve (AUC) function of Prism Graphpad was used for quantification. The standard deviation was calculated using Prism Graphpad and error bars represent one standard deviation from the mean. For comparison of multiple mutants (Figure 7C), one-way ANOVA with Dunnett's test was performed in Prism Graphpad. For the analysis of retrogenic mice, each mouse was considered to be an independent replicate (N=5–6). *P* values were calculated using the unpaired Student's *t* test (two-tailed) in Prism Graphpad. *P* values less than 0.05 were considered to be statistically insignificant.

DATA AND SOFTWARE AVAILABILITY

Imaging data has been deposited with Mendeley Data: http://dx.doi.org/10.17632/xxjvj8yghx.1

Supplementary Material

Refer to Web version on PubMed Central for supplementary material.

Acknowledgments

A.C. was supported by a Robertson Foundation/Cancer Research Institute fellowship and J.A. by a Jane Coffin Childs Fund fellowship. This work was supported in part by the Howard Hughes Medical Institute and the National Institutes of Health (NIH), NIAID PO1 AI091580 (A.W. and J.K.), NIAMS K01 AR06548 (B.A.). We thank Al Roque for assisting with animal husbandry. We also thank the Lim lab at UCSF for providing the pHR vector backbone.

References

Amacher JF, Cushing PR, Brooks L 3rd, Boisguerin P, Madden DR. Stereochemical preferences modulate affinity and selectivity among five PDZ domains that bind CFTR: comparative structural and sequence analyses. Structure. 2014; 22:82–93. [PubMed: 24210758]

Ashkenazy H, Erez E, Martz E, Pupko T, Ben-Tal N. ConSurf 2010: calculating evolutionary conservation in sequence and structure of proteins and nucleic acids. Nucleic Acids Res. 2010; 38:W529–533. [PubMed: 20478830]

Au-Yeung BB, Deindl S, Hsu LY, Palacios EH, Levin SE, Kuriyan J, Weiss A. The structure, regulation, and function of ZAP-70. Immunol Rev. 2009; 228:41–57. [PubMed: 19290920]

Autero M, Saharinen J, Pessa-Morikawa T, Soula-Rothhut M, Oetken C, Gassmann M, Bergman M, Alitalo K, Burn P, Gahmberg CG, et al. Tyrosine phosphorylation of CD45 phosphotyrosine phosphatase by p50csk kinase creates a binding site for p56lck tyrosine kinase and activates the phosphatase. Mol Cell Biol. 1994; 14:1308–1321. [PubMed: 7507203]

Ballek O, Valecka J, Manning J, Filipp D. The pool of preactivated Lck in the initiation of T-cell signaling: a critical re-evaluation of the Lck standby model. Immunol Cell Biol. 2015; 93:384–395. [PubMed: 25420722]

Bergman M, Mustelin T, Oetken C, Partanen J, Flint NA, Amrein KE, Autero M, Burn P, Alitalo K. The human p50csk tyrosine kinase phosphorylates p56lck at Tyr-505 and down regulates its catalytic activity. EMBO J. 1992; 11:2919–2924. [PubMed: 1639064]

Boggon TJ, Eck MJ. Structure and regulation of Src family kinases. Oncogene. 2004; 23:7918–7927. [PubMed: 15489910]

Byth KF, Conroy LA, Howlett S, Smith AJ, May J, Alexander DR, Holmes N. CD45-null transgenic mice reveal a positive regulatory role for CD45 in early thymocyte development, in the selection of CD4+CD8+ thymocytes, and B cell maturation. J Exp Med. 1996; 183:1707–1718. [PubMed: 8666928]

Chakraborty AK, Weiss A. Insights into the initiation of TCR signaling. Nat Immunol. 2014; 15:798–807. [PubMed: 25137454]

Chan AC, Dalton M, Johnson R, Kong GH, Wang T, Thoma R, Kurosaki T. Activation of ZAP-70 kinase activity by phosphorylation of tyrosine 493 is required for lymphocyte antigen receptor function. EMBO J. 1995; 14:2499–2508. [PubMed: 7781602]

Chan AC, Irving BA, Fraser JD, Weiss A. The zeta chain is associated with a tyrosine kinase and upon T-cell antigen receptor stimulation associates with ZAP-70, a 70-kDa tyrosine phosphoprotein. Proc Natl Acad Sci U S A. 1991; 88:9166–9170. [PubMed: 1717999]

Cong L, Ran FA, Cox D, Lin S, Barretto R, Habib N, Hsu PD, Wu X, Jiang W, Marraffini LA, et al. Multiplex genome engineering using CRISPR/Cas systems. Science. 2013; 339:819–823. [PubMed: 23287718]

Couture C, Songyang Z, Jascur T, Williams S, Tailor P, Cantley LC, Mustelin T. Regulation of the Lck SH2 domain by tyrosine phosphorylation. J Biol Chem. 1996; 271:24880–24884. [PubMed: 8798764]

Di Bartolo V, Mege D, Germain V, Pelosi M, Dufour E, Michel F, Magistrelli G, Isacchi A, Acuto O. Tyrosine 319, a newly identified phosphorylation site of ZAP-70, plays a critical role in T cell antigen receptor signaling. J Biol Chem. 1999; 274:6285–6294. [PubMed: 10037717]

Granum S, Sundvold-Gjerstad V, Gopalakrishnan RP, Berge T, Koll L, Abrahamsen G, Sorlie M, Spurkland A. The kinase Itk and the adaptor TSAd change the specificity of the kinase Lck in T cells by promoting the phosphorylation of Tyr192. Sci Signal. 2014; 7:ra118. [PubMed: 25492967]

Jin LL, Wybenga-Groot LE, Tong J, Taylor P, Minden MD, Trudel S, McGlade CJ, Moran MF. Tyrosine phosphorylation of the Lyn Src homology 2 (SH2) domain modulates its binding affinity and specificity. Mol Cell Proteomics. 2015; 14:695–706. [PubMed: 25587033]

Kabouridis PS, Magee AI, Ley SC. S-acylation of LCK protein tyrosine kinase is essential for its signalling function in T lymphocytes. EMBO J. 1997; 16:4983–4998. [PubMed: 9305640]

Kishihara K, Penninger J, Wallace VA, Kundig TM, Kawai K, Wakeham A, Timms E, Pfeffer K, Ohashi PS, Thomas ML, et al. Normal B lymphocyte development but impaired T cell maturation in CD45-exon6 protein tyrosine phosphatase-deficient mice. Cell. 1993; 74:143–156. [PubMed: 8334701]

Koretzky GA, Picus J, Thomas ML, Weiss A. Tyrosine phosphatase CD45 is essential for coupling T-cell antigen receptor to the phosphatidyl inositol pathway. Nature. 1990; 346:66–68. [PubMed: 2164155]

Levin SE, Zhang C, Kadlecek TA, Shokat KM, Weiss A. Inhibition of ZAP-70 kinase activity via an analog-sensitive allele blocks T cell receptor and CD28 superagonist signaling. J Biol Chem. 2008; 283:15419–15430. [PubMed: 18378687]

Li R, Xie DD, Dong JH, Li H, Li KS, Su J, Chen LZ, Xu YF, Wang HM, Gong Z, et al. Molecular mechanism of ERK dephosphorylation by striatal-enriched protein tyrosine phosphatase. J Neurochem. 2014; 128:315–329. [PubMed: 24117863]

Mandl JN, Monteiro JP, Vrisekoop N, Germain RN. T cell-positive selection uses self-ligand binding strength to optimize repertoire recognition of foreign antigens. Immunity. 2013; 38:263–274. [PubMed: 23290521]

Manz BN, Tan YX, Courtney AH, Rutaganira F, Palmer E, Shokat KM, Weiss A. Small molecule inhibition of Csk alters affinity recognition by T cells. Elife. 2015; 4

Moogk D, Zhong S, Yu Z, Liadi I, Rittase W, Fang V, Dougherty J, Perez-Garcia A, Osman I, Zhu C, et al. Constitutive Lck Activity Drives Sensitivity Differences between CD8+ Memory T Cell Subsets. J Immunol. 2016; 197:644–654. [PubMed: 27271569]

Mustelin T, Coggeshall KM, Altman A. Rapid activation of the T-cell tyrosine protein kinase pp56lck by the CD45 phosphotyrosine phosphatase. Proc Natl Acad Sci U S A. 1989; 86:6302–6306. [PubMed: 2548204]

Nada S, Yagi T, Takeda H, Tokunaga T, Nakagawa H, Ikawa Y, Okada M, Aizawa S. Constitutive activation of Src family kinases in mouse embryos that lack Csk. Cell. 1993; 73:1125–1135. [PubMed: 8513497]

Ng DH, Watts JD, Aebersold R, Johnson P. Demonstration of a direct interaction between p56lck and the cytoplasmic domain of CD45 in vitro. J Biol Chem. 1996; 271:1295–1300. [PubMed: 8576115]

Nika K, Soldani C, Salek M, Paster W, Gray A, Etzensperger R, Fugger L, Polzella P, Cerundolo V, Dushek O, et al. Constitutively active Lck kinase in T cells drives antigen receptor signal transduction. Immunity. 2010; 32:766–777. [PubMed: 20541955]

Nika K, Tautz L, Arimura Y, Vang T, Williams S, Mustelin T. A weak Lck tail bite is necessary for Lck function in T cell antigen receptor signaling. J Biol Chem. 2007; 282:36000–36009. [PubMed: 17897955]

Ostergaard HL, Shackelford DA, Hurley TR, Johnson P, Hyman R, Sefton BM, Trowbridge IS. Expression of CD45 alters phosphorylation of the lck-encoded tyrosine protein kinase in murine lymphoma T-cell lines. Proc Natl Acad Sci U S A. 1989; 86:8959–8963. [PubMed: 2530588]

Persaud SP, Parker CR, Lo WL, Weber KS, Allen PM. Intrinsic CD4+ T cell sensitivity and response to a pathogen are set and sustained by avidity for thymic and peripheral complexes of self peptide and MHC. Nat Immunol. 2014; 15:266–274. [PubMed: 24487322]

Philipsen L, Reddycherla AV, Hartig R, Gumz J, Kastle M, Kritikos A, Poltorak MP, Prokazov Y, Turbin E, Weber A, et al. De novo phosphorylation and conformational opening of the tyrosine kinase Lck act in concert to initiate T cell receptor signaling. Sci Signal. 2017:10.

Pingel JT, Thomas ML. Evidence that the leukocyte-common antigen is required for antigen-induced T lymphocyte proliferation. Cell. 1989; 58:1055–1065. [PubMed: 2550143]

Polic B, Kunkel D, Scheffold A, Rajewsky K. How alpha beta T cells deal with induced TCR alpha ablation. Proc Natl Acad Sci U S A. 2001; 98:8744–8749. [PubMed: 11447257]

Ragusa MJ, Dancheck B, Critton DA, Nairn AC, Page R, Peti W. Spinophilin directs protein phosphatase 1 specificity by blocking substrate binding sites. Nat Struct Mol Biol. 2010; 17:459–464. [PubMed: 20305656]

Schmedt C, Saijo K, Niidome T, Kuhn R, Aizawa S, Tarakhovsky A. Csk controls antigen receptor-mediated development and selection of T-lineage cells. Nature. 1998; 394:901–904. [PubMed: 9732874]

Schoenborn JR, Tan YX, Zhang C, Shokat KM, Weiss A. Feedback circuits monitor and adjust basal Lck-dependent events in T cell receptor signaling. Sci Signal. 2011; 4:ra59. [PubMed: 21917715]

Seddon B, Zamoyska R. TCR signals mediated by Src family kinases are essential for the survival of naive T cells. J Immunol. 2002; 169:2997–3005. [PubMed: 12218114]

Shaw AS, Chalupny J, Whitney JA, Hammond C, Amrein KE, Kavathas P, Sefton BM, Rose JK. Short related sequences in the cytoplasmic domains of CD4 and CD8 mediate binding to the amino-terminal domain of the p56lck tyrosine protein kinase. Mol Cell Biol. 1990; 10:1853–1862. [PubMed: 2109184]

Sicheri F, Moarefi I, Kuriyan J. Crystal structure of the Src family tyrosine kinase Hck. Nature. 1997; 385:602–609. [PubMed: 9024658]

Sieh M, Bolen JB, Weiss A. CD45 specifically modulates binding of Lck to a phosphopeptide encompassing the negative regulatory tyrosine of Lck. EMBO J. 1993; 12:315–321. [PubMed: 8428589]

Sjolin-Goodfellow H, Frushicheva MP, Ji Q, Cheng DA, Kadlecek TA, Cantor AJ, Kuriyan J, Chakraborty AK, Salomon AR, Weiss A. The catalytic activity of the kinase ZAP-70 mediates

basal signaling and negative feedback of the T cell receptor pathway. Sci Signal. 2015; 8:ra49. [PubMed: 25990959]

Smith-Garvin JE, Koretzky GA, Jordan MS. T cell activation. Annu Rev Immunol. 2009; 27:591–619. [PubMed: 19132916]

Soula M, Rothhut B, Camoin L, Guillaume JL, Strosberg D, Vorherr T, Burn P, Meggio F, Fischer S, Fagard R. Anti-CD3 and phorbol ester induce distinct phosphorylated sites in the SH2 domain of p56lck. J Biol Chem. 1993; 268:27420–27427. [PubMed: 8262984]

Stirnweiss A, Hartig R, Gieseler S, Lindquist JA, Reichardt P, Philipsen L, Simeoni L, Poltorak M, Merten C, Zuschratter W, et al. T cell activation results in conformational changes in the Src family kinase Lck to induce its activation. Sci Signal. 2013; 6:ra13. [PubMed: 23423439]

Stover DR, Furet P, Lydon NB. Modulation of the SH2 binding specificity and kinase activity of Src by tyrosine phosphorylation within its SH2 domain. J Biol Chem. 1996; 271:12481–12487. [PubMed: 8647855]

Szymczak AL, Workman CJ, Wang Y, Vignali KM, Dilioglou S, Vanin EF, Vignali DA. Correction of multi-gene deficiency in vivo using a single 'self-cleaving' 2A peptide-based retroviral vector. Nat Biotechnol. 2004; 22:589–594. [PubMed: 15064769]

Tan YX, Manz BN, Freedman TS, Zhang C, Shokat KM, Weiss A. Inhibition of the kinase Csk in thymocytes reveals a requirement for actin remodeling in the initiation of full TCR signaling. Nat Immunol. 2014; 15:186–194. [PubMed: 24317039]

Tong L, Warren TC, King J, Betageri R, Rose J, Jakes S. Crystal structures of the human p56lck SH2 domain in complex with two short phosphotyrosyl peptides at 1.0 A and 1.8 A resolution. J Mol Biol. 1996; 256:601–610. [PubMed: 8604142]

van Oers NS, Killeen N, Weiss A. ZAP-70 is constitutively associated with tyrosine-phosphorylated TCR zeta in murine thymocytes and lymph node T cells. Immunity. 1994; 1:675–685. [PubMed: 7600293]

van Oers NS, Lowin-Kropf B, Finlay D, Connolly K, Weiss A. alpha beta T cell development is abolished in mice lacking both Lck and Fyn protein tyrosine kinases. Immunity. 1996; 5:429–436. [PubMed: 8934570]

Vouilleme L, Cushing PR, Volkmer R, Madden DR, Boisguerin P. Engineering peptide inhibitors to overcome PDZ binding promiscuity. Angew Chem Int Ed Engl. 2010; 49:9912–9916. [PubMed: 21105032]

Williams BL, Irvin BJ, Sutor SL, Chini CC, Yacyshyn E, Bubeck Wardenburg J, Dalton M, Chan AC, Abraham RT. Phosphorylation of Tyr319 in ZAP-70 is required for T-cell antigen receptor-dependent phospholipase C-gamma1 and Ras activation. EMBO J. 1999; 18:1832–1844. [PubMed: 10202147]

Xu W, Harrison SC, Eck MJ. Three-dimensional structure of the tyrosine kinase c-Src. Nature. 1997; 385:595–602. [PubMed: 9024657]

Yamaguchi H, Hendrickson WA. Structural basis for activation of human lymphocyte kinase Lck upon tyrosine phosphorylation. Nature. 1996; 384:484–489. [PubMed: 8945479]

Zhang W, Sloan-Lancaster J, Kitchen J, Trible RP, Samelson LE. LAT: the ZAP-70 tyrosine kinase substrate that links T cell receptor to cellular activation. Cell. 1998; 92:83–92. [PubMed: 9489702]

Zhu JW, Doan K, Park J, Chau AH, Zhang H, Lowell CA, Weiss A. Receptor-like tyrosine phosphatases CD45 and CD148 have distinct functions in chemoattractant-mediated neutrophil migration and response to S. aureus. Immunity. 2011; 35:757–769. [PubMed: 22078799]

Zikherman J, Jenne C, Watson S, Doan K, Raschke W, Goodnow CC, Weiss A. CD45-Csk phosphatase-kinase titration uncouples basal and inducible T cell receptor signaling during thymic development. Immunity. 2010; 32:342–354. [PubMed: 20346773]

HIGHLIGHTS

- T cell maturation is impaired in retrogenic mice harboring a Lck Y192 mutation
- Y192 modification disrupts the ability of CD45 to associate with Lck and activate it
- By disrupting Lck activation the Y192 phosphosite can inhibit TCR signaling
- A Zap70-dependent negative feedback loop is proposed to regulate active Lck levels

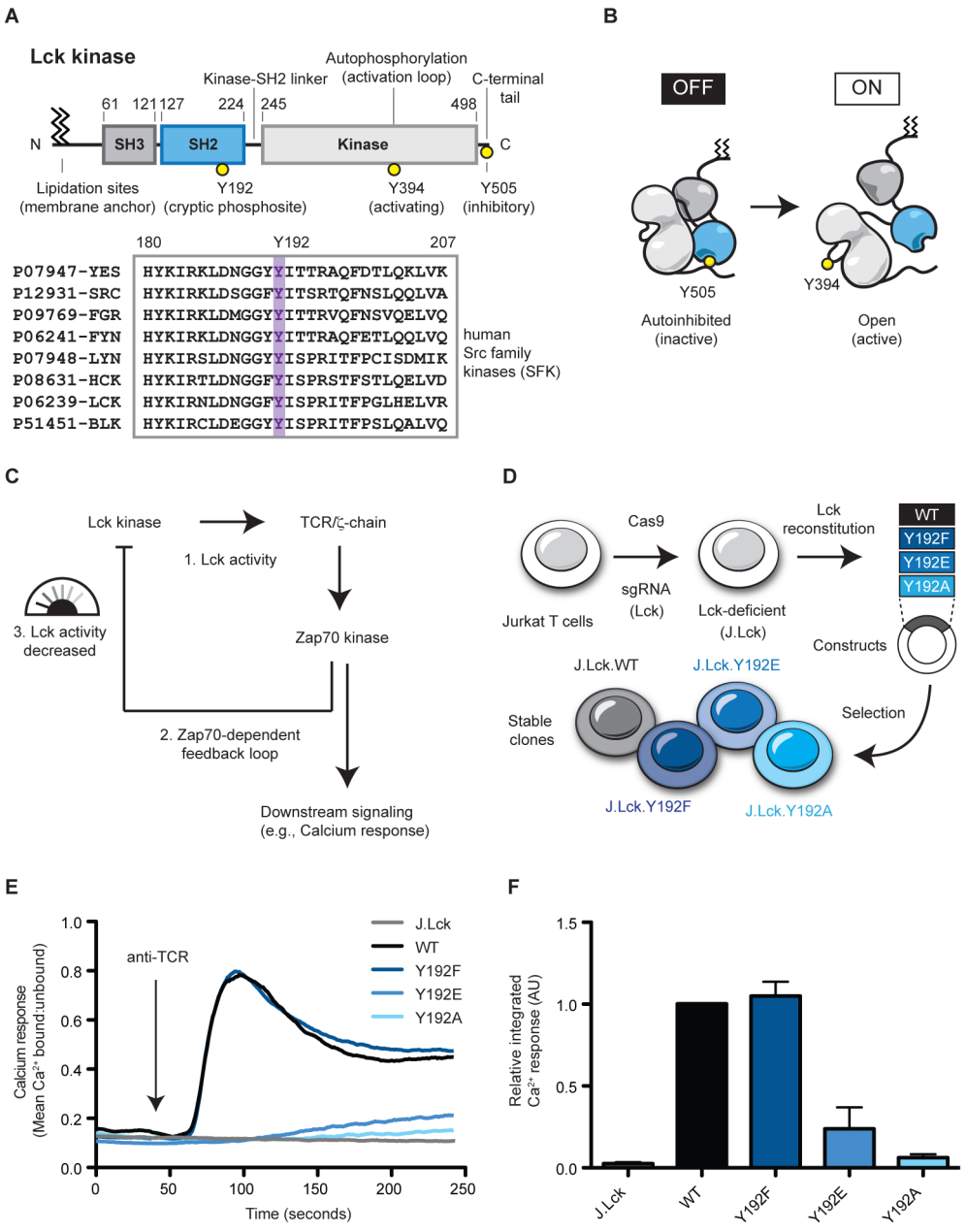

Figure 1.

Targeted deletion of Lck and reconstitution with Lck Y192 variants reveals a signaling defect. (A) Lck, a Src family kinase (SFK), possess two regulatory domains and several sites of post-translational modification. (B) Lck kinase activity is controlled by its conformation which is regulated by phosphorylation. (C) Proposed Zap70-dependent negative feedback loop. (D) Schematic for stable reconstitution of Lck-deficient Jurkat T cells. (E) Intracellular calcium influx in response to TCR stimulation was assessed by flow cytometry. After a 40 second baseline, cells were stimulated with anti-TCR antibody. (F) Calcium responses were integrated and quantified relative to WT Lck. Error bars represent ± one SD from the mean (N=3). See also Figures S1&S2.

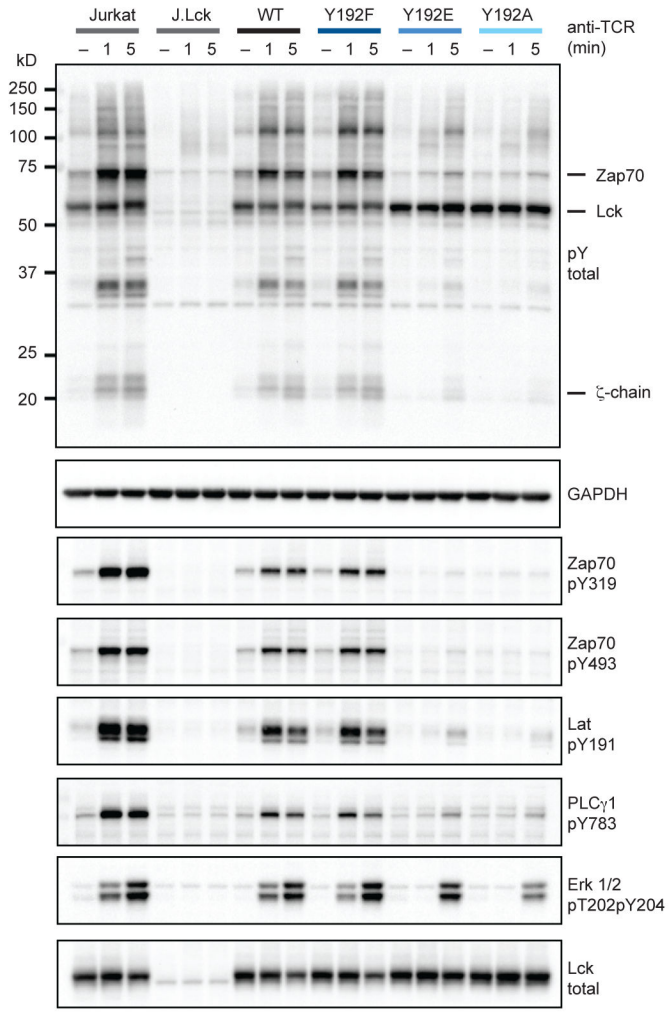

Figure 2.

TCR stimulation induced protein phosphorylation is attenuated by Y192 mutation. Resting Jurkat T cells and J.Lck cells reconstituted with Lck variants were stimulated with anti-TCR antibody and lysed at discrete intervals. Immunoblot analysis was carried out with a pan-phosphotyrosine (pY) antibody to reveal changes in total protein tyrosine phosphorylation. The MW of key signaling components are denoted. Phosphospecific antibodies were used to assess the activation status of specific proteins. Data are representative of three independent experiments. See also Figure S2.

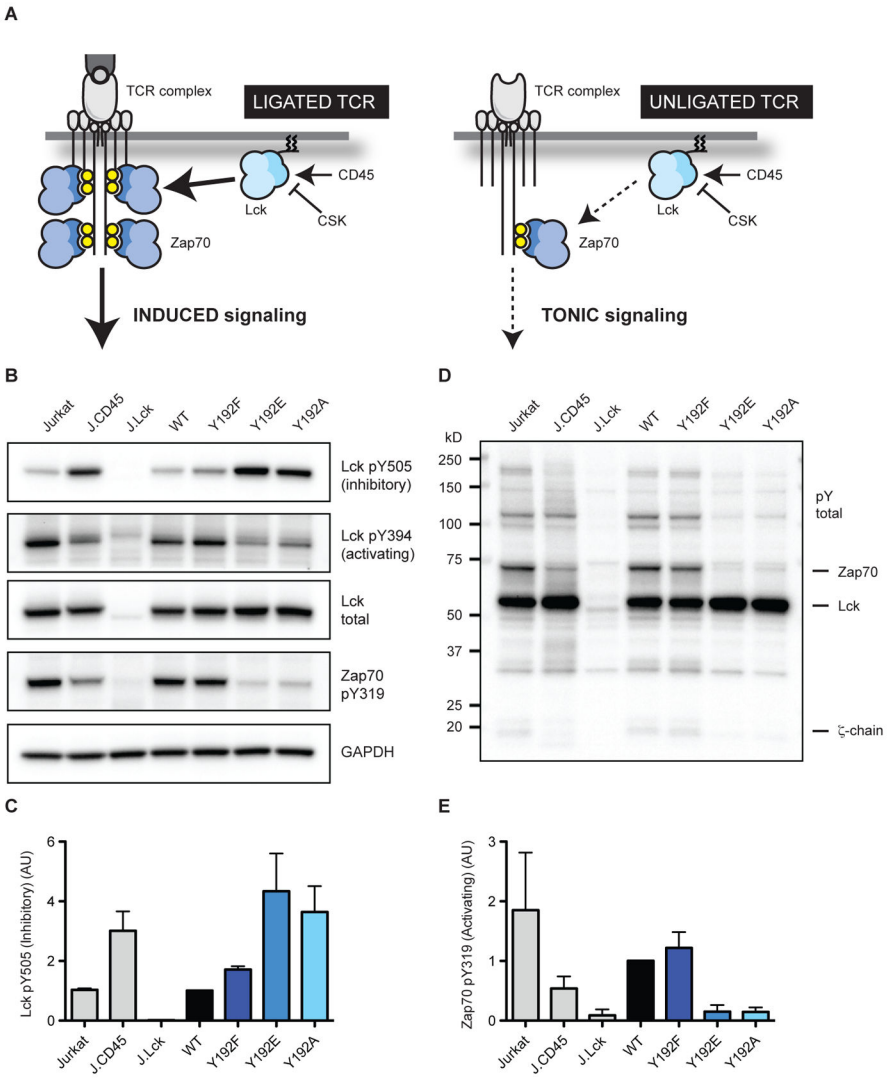

Figure 3.

Y192 regulates Lck kinase activity and tonic TCR signaling. (A) Inducible TCR signaling occurs upon antigen binding or agonists such as anti-TCR antibodies. Tonic signaling occurs constitutively through the TCR in the absence of ligand. (B) Resting Jurkat T cells, CD45-deficient J.CD45 cells, and J.Lck variants were lysed. Lysates were probed by immunoblot to assess basal phosphorylation. (C) Phosphorylation of the inhibitory C-terminal tail (Y505) was normalized to WT Lck and quantified. (D) Total protein phosphotyrosine abundance was assessed by immunoblot, the MW of key signaling components are denoted. (E) Zap70 phosphorylation was quantified as a readout of tonic TCR signaling. Error bars represent ± one SD from the mean (N=3).

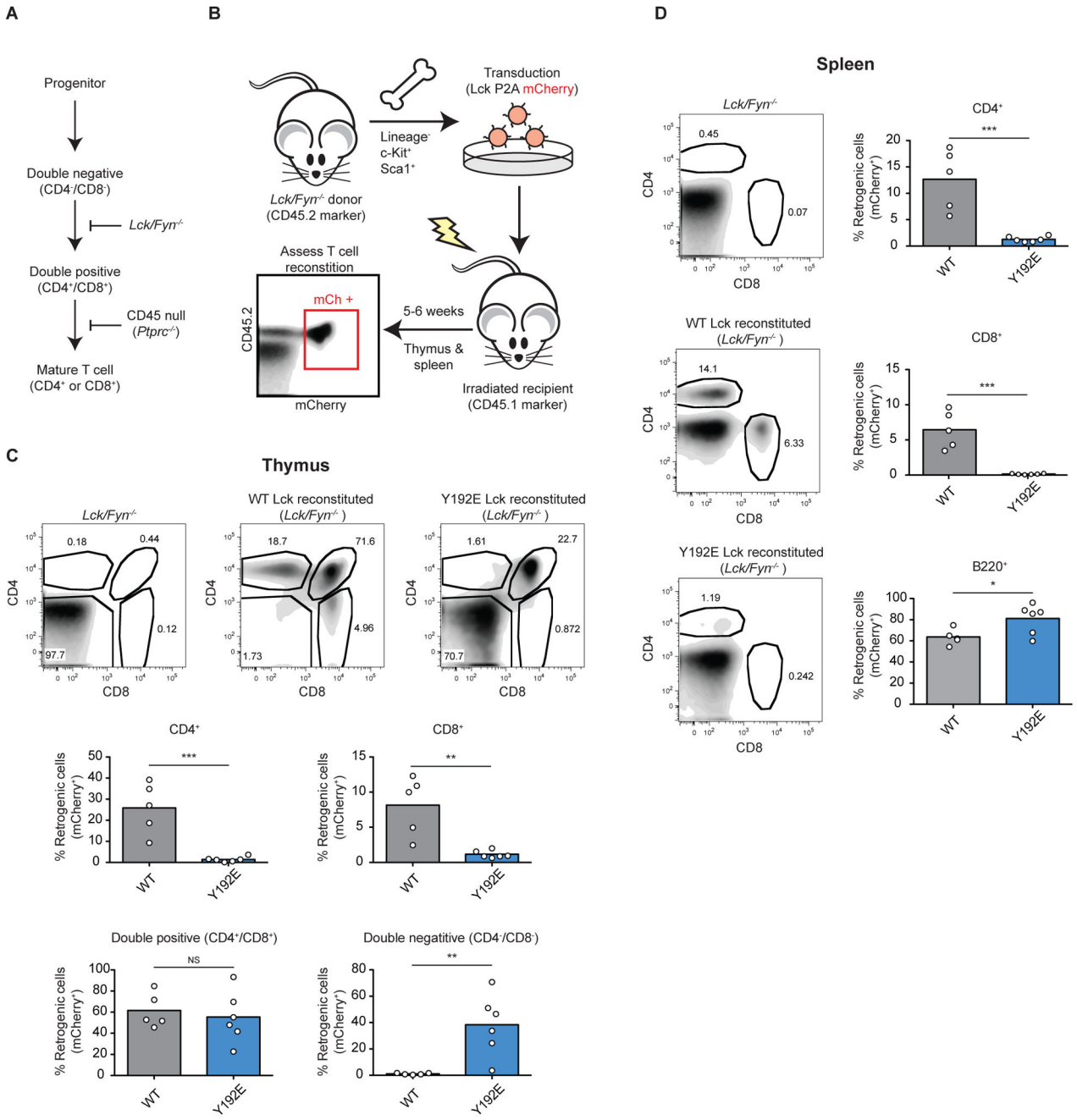

Figure 4.

Thymic reconstitution of retrogenic mice harboring a Y192 mutation is impaired. (A) Schematic for the maturation of thymocytes during T cell development. Deletion of SFKs Lck/Fyn prevents maturation of double negative thymocytes. Deletion of CD45 prevents positive selection of double positive ($CD4^+/CD8^+$) thymocytes. (B) Hematopoetic progenitor cells were isolated from Lck/Fyn-deficient bone marrow and transduced with WT Lck or the Y192E variant. Transduced precursors were transferred into conjenically marked lethally irradiated mice (CD45.1). (C) Retrogenic thymocytes ($mCherry^+/CD45.2^+$) were assessed for CD4 and CD8 expression to identify thymocyte populations: double negative

($CD4^-/CD8^-$), double positive ($CD4^+/CD8^+$) and mature single positive ($CD4^+$ or $CD8^+$). Populations were quantified as a percentage of total retrogenic thymocytes. (D) Spleens were similarly assessed for mature CD4 and CD8 single positive T cells and B cells ($B220^+$). * $P \leq 0.05$, ** $P < 0.01$, *** $P < 0.001$, and NS $P > 0.05$. *P* values were calculated using the unpaired Student's *t* test (N=5 or 6 mice per group). See also Figure S3.

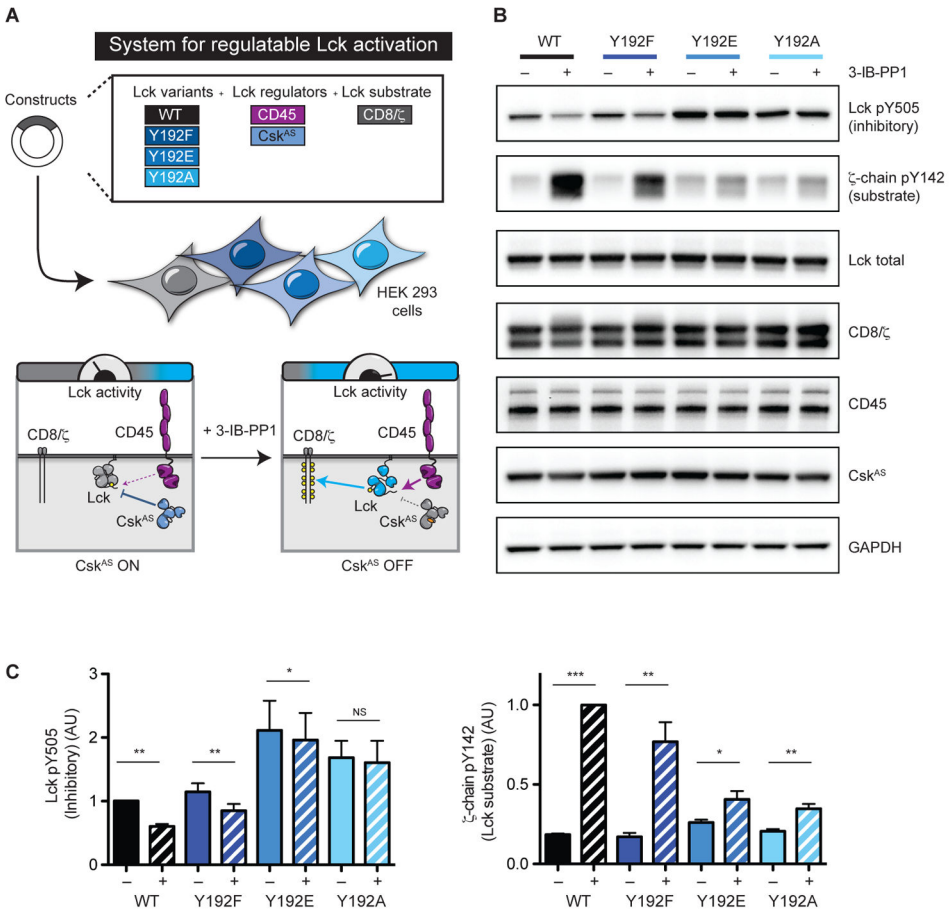

Figure 5.

Regulatable activation of Lck reveals a defect in CD45-mediated activation of Y192 variants. (A) A reconstituted cellular system for Lck activation in HEK 293 cells. Addition of 3-IB-PP1 inhibits Csk^{AS} which phosphorylates the inhibitory C-terminal tail (Y505). Increased Lck activity results in phosphorylation of an Lck substrate, CD8/ζ-chain. (B) Resting HEK 293 cells were treated with either DMSO or 3-IB-PP1 (5 μM) and lysed. Lysates were assessed by immunoblot for C-terminal tail (Y505) and CD8/ζ-chain phosphorylation. (C) Quantification of immunoblots relative to WT Lck. Error bars represent ± one SD from the mean (N=3). * $P \leq 0.05$, ** $P < 0.01$, *** $P < 0.001$, and NS P > 0.05. *P* values were calculated using the paired Student's *t* test.

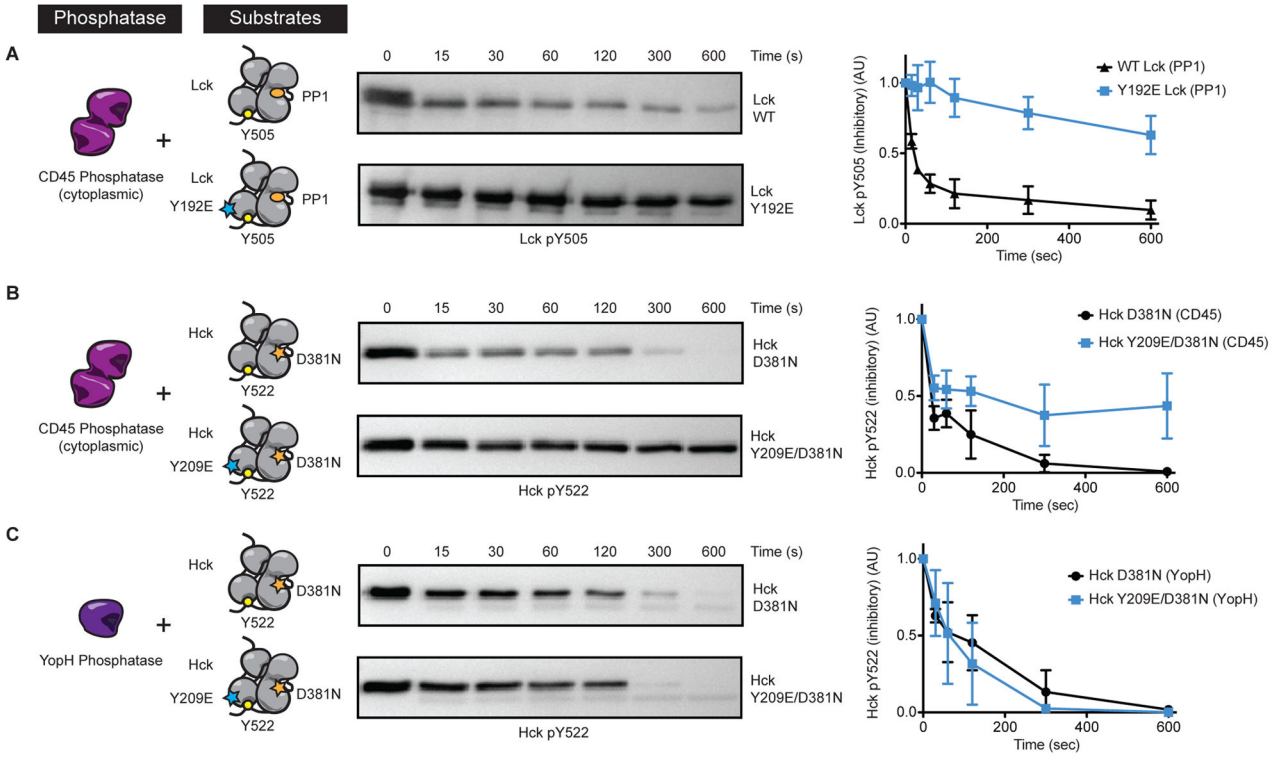

Figure 6.

Lck Y192 and Hck Y209 directly mediate dephosphorylation of the inhibitory C-terminal tail by CD45. (A) Purified Lck was inhibited with PP1 and treated with the cytoplasmic domain of the phosphatase CD45. Dephosphorylation of the C-terminal tail (Y505) was assessed by immunoblot and quantified (*right panel*). (B) Autoinhibited catalytically inactive (D381) Hck, and the Y209E variant, were treated with the cytoplasmic domain of CD45, or (C) the promiscuous phosphatase YopH, and dephosphorylation of the C-terminal tail (Y522) quantified (*right panels*). Error bars represent ± one SD from the mean (N=3). See also Figure S5.

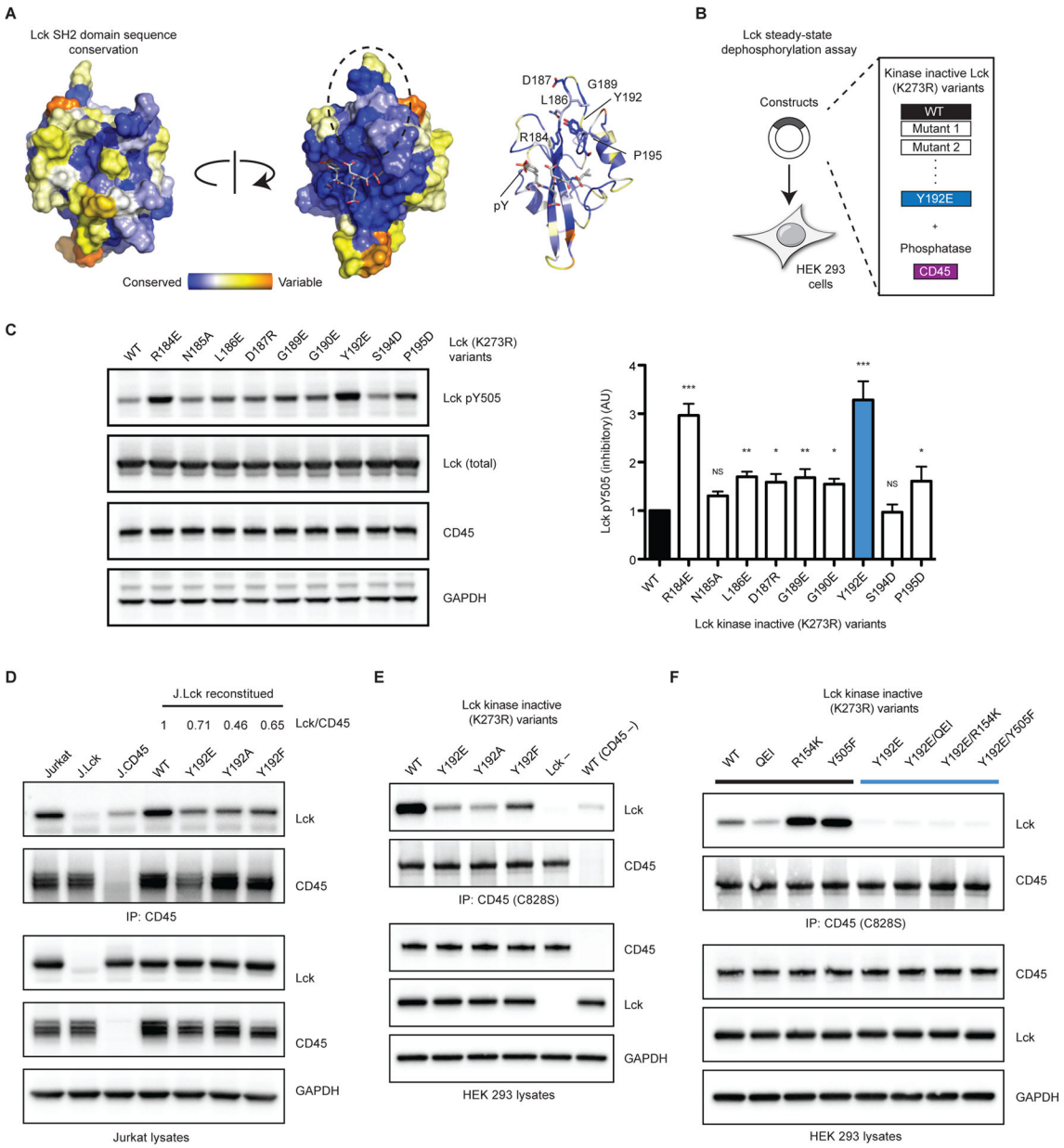

Figure 7.

A docking site located within the SH2 domain of Lck mediates association with CD45 and dephosphorylation of the C-terminal tail. (A) Residues adjacent to Y192 comprise a conserved region (dotted circle). (B) The capacity of CD45 to dephosphorylate the C-terminal tail (Y505) of Lck variants was assessed in a steady-state dephosphorylation assay. (C) Immunoblot analysis of Lck Y505 dephosphorylation by CD45 and quantification. (D) CD45 was immunoprecipitated from J.Lck variants and associated Lck assessed by immunoblot. Quantification of Lck to CD45 ratio from IP is denoted. (E) HEK 293 cells were transfected with inactive CD45 (C828S) and inactive Lck (K273R) variants. CD45 was immunoprecipitated and associated Lck assessed by immunoblot. (F) Additional mutations were incorporated into catalytically inactive Lck. QEI stabilizes the autoinhibited

conformation, whereas both R154K and Y505F disrupt the autoinhibited conformation. Data are representative of three independent experiments. * $P \leq 0.05$, ** $P < 0.01$, *** $P < 0.001$, and NS $P > 0.05$. P values were calculated using one-way ANOVA (Dunnett test) (N=3). See also Figures S6 & S7, and STAR methods.